Materials Advances

ROYAL SOCIETY OF CHEMISTRY

COMMUNICATION

View Article Online
View Journal | View Issue

Cite this: *Mater. Adv.*, 2021, 2, 3257

Received 15th December 2020, Accepted 23rd March 2021

DOI: 10.1039/d0ma00983k

rsc.li/materials-advances

Experimental validation of high electrical conductivity in Ni-rich $LaNi_{1-x}Fe_xO_3$ solid solutions ($x \leq 0.4$) in high-temperature oxidizing atmospheres†

Yoshinobu Adachi,‡[a] Naoyuki Hatada,*[a] Masaki Kato,[b] Ken Hirota[b] and Tetsuya Uda*[a]

$LaNi_{1-x}Fe_xO_3$ solid solutions are an interesting system exhibiting a composition-controlled metal–insulator transition and are also potential cathode materials for solid oxide fuel cells, but the composition dependence of their electrical conductivity is still an open question due to the difficulty in synthesis and sintering. Here, in contrast to previous studies, it is demonstrated that the electrical conductivity of $LaNi_{1-x}Fe_xO_3$ monotonically increases with decreasing x (increasing Ni content), reaching as high as 1.0×10^4 S cm^{-1} at room temperature and 2.5×10^3 S cm^{-1} at 800 °C in 0.2 bar O_2 when $x = 0$. The accurate electrical conductivity measurements of $LaNi_{1-x}Fe_xO_3$ with high Ni contents ($0 \leq x \leq 0.4$) are realized using fully dense single-phase polycrystalline samples prepared by the post-sintering oxidation process. The results suggest that $LaNi_{1-x}Fe_xO_3$ with a higher Ni content might be more suitable as the cathodes than the widely-studied composition $LaNi_{0.6}Fe_{0.4}O_3$. Furthermore, $LaNiO_3$ is now considered to have the highest electrical conductivity among precious-metal-free oxides in high-temperature oxidizing atmospheres and can find more applications.

$LaNiO_3$, $LaFeO_3$, and their solid solutions $LaNi_{1-x}Fe_xO_3$ (LNF, $0 \leq x \leq 1$) have been extensively studied in the field of solid state chemistry/physics for over 50 years owing to their interesting electrical properties.[1–21] $LaNiO_3$ is a metallic oxide with high electrical conductivity, which is rather unusual for undoped 3d-transition-metal-based perovskite oxides.[6,10] $LaNiO_3$ contains a low-spin configuration of Ni^{3+} ($t_{2g}^6e_g^1$).[1,7,8,11] Due to the strong covalent bonding between Ni^{3+} and O^{2-}, the e_g orbitals are transformed into one-quarter filled itinerant σ* band states, and it results in the metallic behaviors. By contrast, $LaFeO_3$ is a charge-transfer insulator which contains a high-spin, localized electron configuration of Fe^{3+} ($t_{2g}^3e_g^2$).[1,11] Consequently the $LaNi_{1-x}Fe_xO_3$ system exhibits a composition-controlled metal–insulator (m–i) transition at $x = \sim 0.3$.[2,3,5,12–14,22,23] Although no existing theory is sufficient to describe entirely the evolution of the electronic structure across the transition, a number of experimental and theoretical studies suggest that the metal–insulator transition is driven by increasing disorder effects arising from the random substitution for Ni with Fe in a metallic system with long-range Coulomb interactions.[12,16]

In recent decades, $LaNi_{1-x}Fe_xO_3$ (in particular $x = 0.4$) has also been recognized as a promising cathode material for solid oxide fuel cells (SOFCs)[22–42] because of its high electrical conductivity,[22–26,28,32,34,37] good catalytic activity for oxygen reduction reaction,[24,27,29,40] high durability against chromium poisoning,[30] and thermal expansion coefficient (TEC) close to those of typical electrolyte materials.[24–26,28,31–33,37]

Here, the structural and physical properties of $LaNi_{1-x}Fe_xO_3$ is briefly reviewed, which vary rather monotonically with iron content x. At room temperature, the solid solutions with $0 \leq x < 0.5$ are isostructural with $LaNiO_3$ and have a rhombohedral perovskite structure, while those with composition $0.5 < x \leq 1$ are isostructural with $LaFeO_3$ and have an orthorhombic perovskite structure.[2,14,15,20,22,24,31,32,43,44] At 800 °C, the stable region of the rhombohedral phase extends up to $x = \sim 0.9$.[31] The molar volume of $LaNi_{1-x}Fe_xO_3$ increases with x due to the larger ionic radius of Fe^{3+} compared with that of Ni^{3+}.[14,15,22,24,31,32,33,38,43] The thermal expansion coefficient is normally reported to be in the range of $8–14 \times 10^{-6}$ K^{-1}, close to those of typical electrolyte materials yttrium-stabilized zirconia (YSZ) and gadolinium-doped ceria (GDC), and it decreases with x.[24–26,28,31–33,37] $LaNiO_3$ decompose in air at around 1000 °C or higher to form phases with oxidation states of Ni below +3 according to the following equation:[45]

$$4LaNiO_3\ (s) \rightarrow La_4Ni_3O_{10}\ (s) + NiO\ (s) + 1/2O_2\ (g) \quad (1)$$

[a] *Department of Materials Science and Engineering, Kyoto University, Yoshida-honmachi, Sakyo-ku, Kyoto 606-8501, Japan. E-mail: hatada.naoyuki.8u@kyoto-u.jp, uda.tetsuya.5e@kyoto-u.ac.jp*

[b] *Department of Molecular Chemistry and Biochemistry, Faculty of Science and Engineering, Doshisha University, Kyo-Tanabe, Kyoto 610-0321, Japan*

† Electronic supplementary information (ESI) available: Experimental details, oxygen partial pressure dependence of the electrical conductivity of $LaNi_{1-x}Fe_xO_3$, thermodynamic stability of lanthanum nickelates. See DOI: 10.1039/d0ma00983k

‡ Deceased.

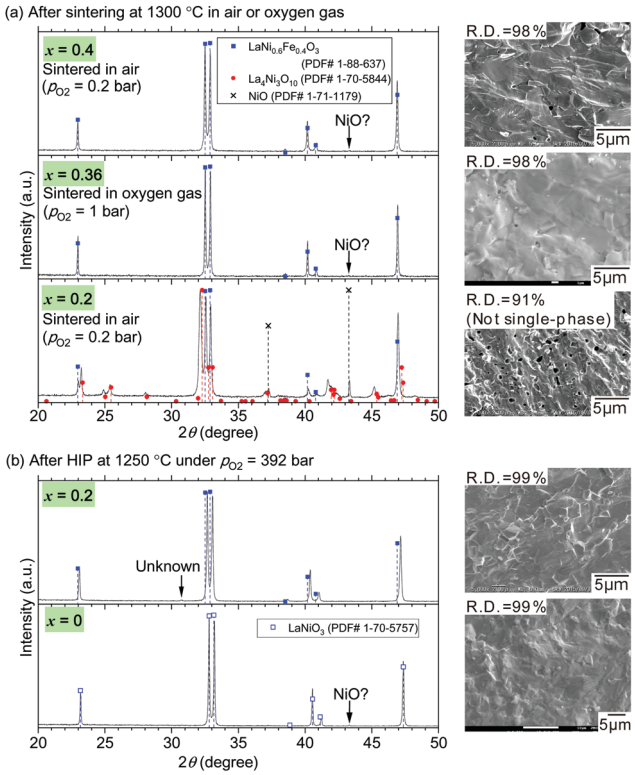

Fig. 1 Powder X-ray diffraction patterns and SEM images of $LaNi_{1-x}Fe_xO_3$ tablets (a) after sintered at 1300 °C in air or oxygen gas and (b) after HIP treatments at 1250 °C under p_{O_2} = 392 bar. The SEM images are those of fracture surfaces of the tablets. Their relative densities measured by the Archimedes method are indicated on the SEM images. The data of $LaNi_{1-x}Fe_xO_3$ with x = 0 are from our previous work.[46] Part of the figure was presented at conferences.[47,48]

This makes synthesis and sintering of $LaNiO_3$ difficult. The decomposition temperature of $LaNi_{1-x}Fe_xO_3$ becomes higher with x due to the higher stability of Fe^{3+} compared with Ni^{3+}, and thus $LaNi_{0.6}Fe_{0.4}O_3$ (x = 0.4) is stable up to around 1200 °C in air.[15,22,38,43,44]

Despite many works to characterize $LaNi_{1-x}Fe_xO_3$, the composition dependence of the electrical conductivity of $LaNi_{1-x}Fe_xO_3$ is still an open question. Some studies have shown a monotonic increase of the electrical conductivity with decreasing x (increasing Ni content),[3,12,13,28] while other recent studies have indicated a conductivity maximum at x = 0.4.[19,22,24,32] The overpotential of $LaNi_{1-x}Fe_xO_3$ cathodes on scandia-stabilized zirconia electrolytes reached a minimum also at x = 0.4, which suggested a correlation between the electrical conductivity and the cathode performance.[24] Based on this, most of the studies aiming at the development of $LaNi_{1-x}Fe_xO_3$ cathodes for SOFCs have focused on $LaNi_{1-x}Fe_xO_3$ with x = 0.4.[26,27,29,33,34,36,37,40,41] However, it is worth mentioning that the decrease in the electrical conductivity while entering into the metallic region ($x < \sim 0.3$) is rather unusual. In this context, the origin of the apparent conductivity maximum has been suggested to be lower sintering density[22] or decomposition[24,32] of $LaNi_{1-x}Fe_xO_3$ samples with $x < 0.4$ due to their poor thermal stability. Therefore, it is quite important to re-evaluate accurately the electrical conductivity of

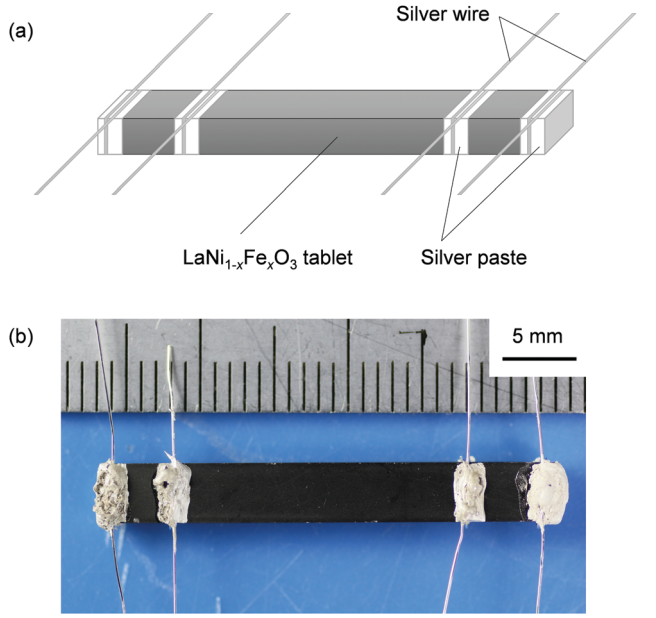

Fig. 2 (a) Schematic of $LaNi_{1-x}Fe_xO_3$ samples used for electrical conductivity measurements. (b) Photograph of a $LaNi_{0.6}Fe_{0.4}O_3$ sample used for electrical conductivity measurements.

$LaNi_{1-x}Fe_xO_3$ with $x < 0.4$ to validate the picture of the electronic conduction in the $LaNi_{1-x}Fe_xO_3$ system and to find the optimal composition as cathodes.

In this study, we have prepared dense polycrystalline samples of single-phase $LaNi_{1-x}Fe_xO_3$ with high Ni contents ($0 \leq x \leq 0.4$) by virtue of the post-sintering oxidation process.[46] In this process, pre-sintered dense tablets of mixed oxides were converted to single-phase $LaNi_{1-x}Fe_xO_3$ under high oxygen partial pressures. Then their accurate electrical conductivity has been evaluated to reveal the composition dependence.

Dense samples of $LaNi_{1-x}Fe_xO_3$ with x = 0.4 and 0.36 were readily prepared by conventional solid-state reaction of La_2O_3, NiO, and Fe_2O_3 and sintering under ordinary pressure, while that with x = 0.2 could not be obtained in the same way. Fig. 1(a) shows powder X-ray diffraction patterns and SEM images of $LaNi_{1-x}Fe_xO_3$ tablets with compositions x = 0.4, 0.36, and 0.2 after sintered at 1300 °C in air, oxygen gas, and air, respectively. The sintered tablets with x = 0.4 and 0.36 were almost single-phase perovskite, while the tablet with x = 0.2 contained impurity phases $La_4Ni_3O_{10}$ and NiO in addition to the perovskite phase.§ The upper temperature limit of the stability of the perovskite phase $LaNi_{1-x}Fe_xO_3$ has been reported to become lower as x or oxygen partial pressure (p_{O_2}) decreases.[38,44] The present results follow this trend and reconfirm the difficulty in sintering $LaNi_{1-x}Fe_xO_3$ with high Ni contents ($x \leq 0.2$) under ordinary pressure.

The post-sintering oxidation realized dense samples of $LaNi_{1-x}Fe_xO_3$ with x = 0.2 and 0. The above mixed-phase tablet with x = 0.2 was subsequently oxidized at 1250 °C under p_{O_2} = 392 bar using hot isostatic pressing (HIP). As evident from its powder X-ray diffraction pattern in Fig. 1(b), the sample with x = 0.2 was converted to almost single-phase perovskite owing

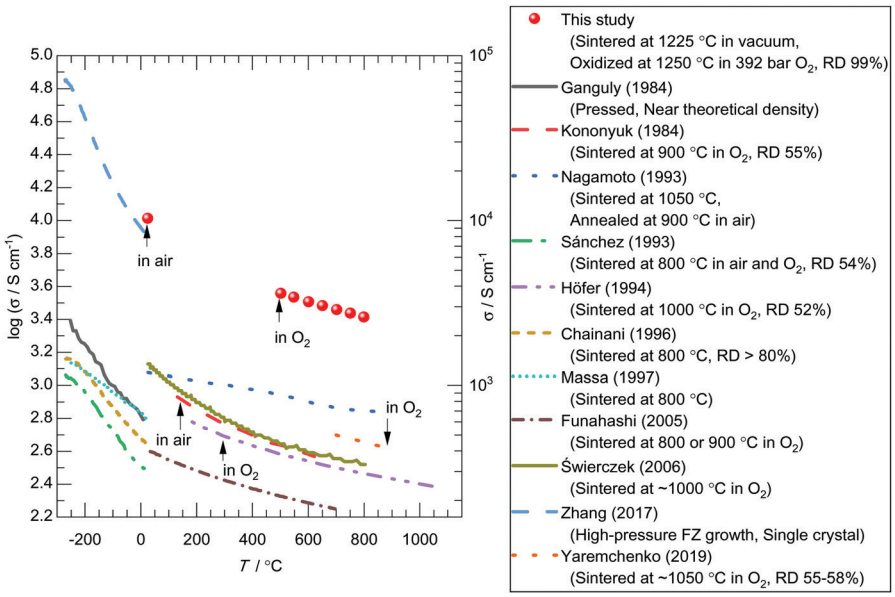

Fig. 3 Temperature dependence of the electrical conductivity (σ) of $LaNiO_3$ measured using a dense sample in this study or published in the literature.[5,12,14,18,28,49–54] Atmospheres where measurements were carried out are indicated in the figure. Preparation conditions and relative densities of the specimen are summarized in the legend. The sintering condition of Świerczek *et al.*[28] was given in their paper as "1000–1200 °C range, depending on the sample chemical composition". As $LaNiO_3$ is considered to be thermally most unstable composition in their paper, we guess the sintering temperature of $LaNiO_3$ was approximately 1000 °C.

to this high-pressure oxidation treatment. A dense sample of single-phase $LaNiO_3$ (x = 0) was also obtained similarly by oxidizing a pre-sintered tablet composed of fine La_2NiO_4 and NiO grains as reported in our previous paper.[46] Its XRD pattern in Fig. 1(b) confirms the almost single-phase nature. SEM images of the fracture surfaces of the samples with x = 0, 0.2, 0.36, and 0.4, and their relative densities measured by the Archimedes method are also shown in Fig. 1(a) and (b). There are few pores in their fracture surfaces after the final heat treatments, and their relative densities finally exceeded 98%.

Electrical conductivity measurements using the dense $LaNiO_3$ sample revealed that the electrical conductivity of $LaNiO_3$ has been much underestimated in the literature due to insufficient sintering. The electrical conductivity measurements of $LaNi_{1-x}Fe_xO_3$ were carried out by the four-probe technique using bar-like tablets with silver electrodes (illustrated in Fig. 2) in air or a mixture of O_2 and Ar gases. Fig. 3 shows the electrical conductivity values of $LaNiO_3$ either obtained in this study using the dense sample or reported in the literature.[5,12,14,18,28,49,50,51,52,53,54] While the temperature

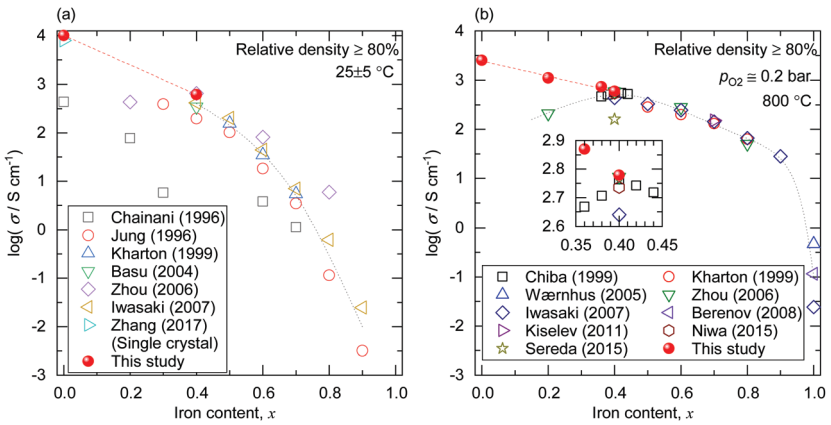

Fig. 4 (a) Iron content dependence of the electrical conductivity of $LaNi_{1-x}Fe_xO_3$ at 25 ± 5 °C. The literature values by Chainani *et al.*,[12] Jung and Iguchi,[13] Kharton *et al.*,[25] Basu *et al.*,[26] Zhou *et al.*,[19] Iwasaki *et al.*,[20] and Zhang *et al.*[53] are also shown. The figure shows only the electrical conductivities of the samples whose relative densities were over 80% or that of a single crystal.[53] (b) Iron content dependence of the electrical conductivity of $LaNi_{1-x}Fe_xO_3$ at 800 °C. The literature values by Chiba *et al.*,[32] Kharton *et al.*,[25] Wærnhus *et al.*,[57] Zhou *et al.*,[19] Iwasaki *et al.*,[20] Berenov *et al.*,[58] Kiselev and Cherepanov,[59] Niwa *et al.*,[23] and Sereda *et al.*[37] are also shown. The figure shows only the electrical conductivities of the samples whose relative densities were over 80%. The inset shows a zoom around x = 0.4. Part of the figure was presented at a conference.[47]

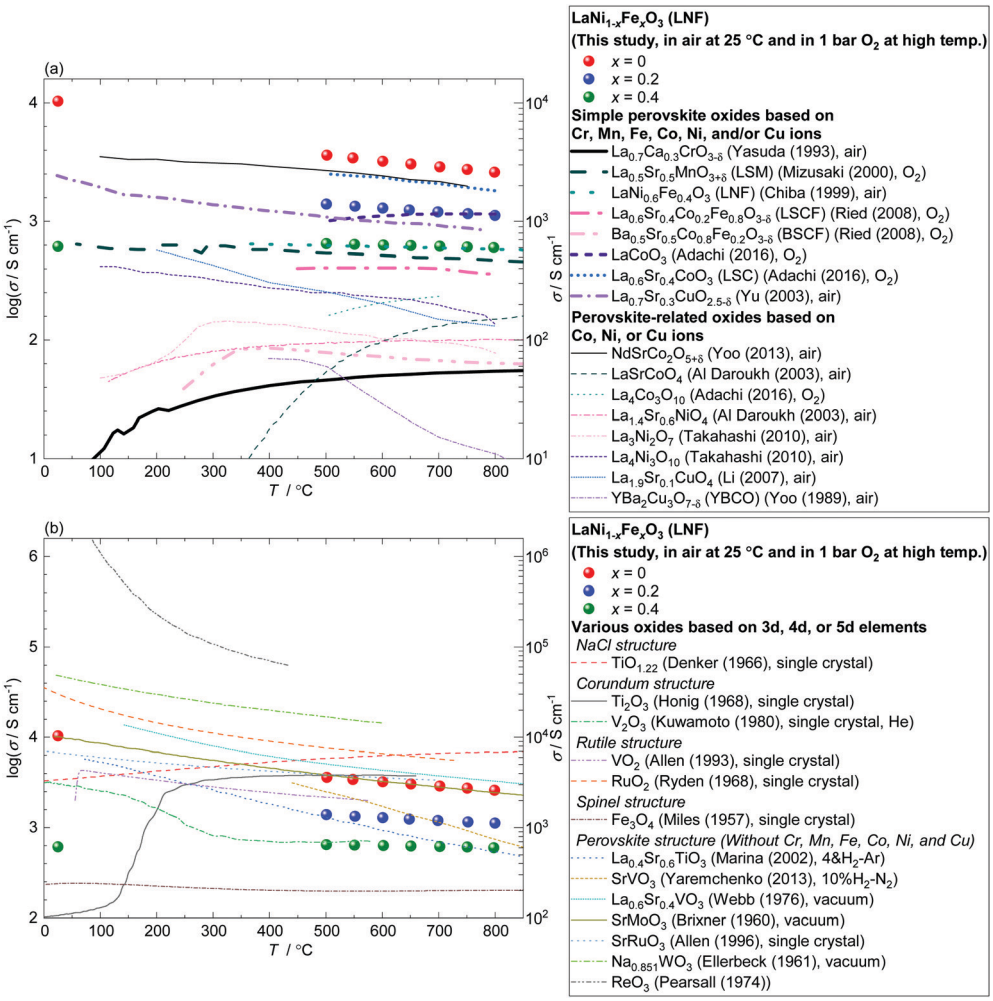

Fig. 5 Comparison of the electrical conductivities of $LaNi_{1-x}Fe_xO_3$ (x = 0, 0.2, 0.4) with those of representative electrically conducting oxides at temperatures between room temperature and 800 °C. Measurement conditions are summarized in the legend. (a) Comparison with simple perovskite or perovskite-related oxides based on 3d transition metals Cr, Mn, Fe, Co, Ni, and/or Cu: $La_{0.7}Ca_{0.3}CrO_{3-\delta}$,[67] $La_{0.5}Sr_{0.5}MnO_{3+\delta}$,[68] $LaNi_{0.6}Fe_{0.4}O_3$,[32] $La_{0.6}Sr_{0.4}Co_{0.2}Fe_{0.8}O_{3-\delta}$,[69] $Ba_{0.5}Sr_{0.5}Co_{0.8}Fe_{0.2}O_{3-\delta}$,[69] $LaCoO_3$,[70] $La_{0.6}Sr_{0.4}CoO_{3-\delta}$,[70] $La_{0.7}Sr_{0.3}CuO_{2.5-\delta}$,[71] $NdSrCo_2O_{5+\delta}$,[72] $LaSrCoO_4$,[73] $La_4Co_3O_{10}$,[70] $La_{1.4}Sr_{0.6}NiO_4$,[73] $La_3Ni_2O_7$,[74] $La_4Ni_3O_{10}$,[74] $La_{1.9}Sr_{0.1}CuO_4$,[75] and $YBa_2Cu_3O_{7-\delta}$.[76] (b) Comparison with other representative electrically conducting oxides out of the above category, based on 3d, 4d, or 5d transition metals: $TiO_{1.22}$,[77] Ti_2O_3,[78] V_2O_3,[79] VO_2,[80] RuO_2,[81] Fe_3O_4,[82] $La_{0.4}Sr_{0.6}TiO_3$,[83] $SrVO_3$,[84] $La_{0.6}Sr_{0.4}VO_3$,[85] $SrMoO_3$,[86] $SrRuO_3$,[87] $Na_{0.851}WO_3$,[88] and ReO_3.[89] Part of the figure was presented at a conference.[48]

dependences (or the slopes) of the present and the reported data are consistent, significant discrepancies are seen in the electrical conductivity values. The present data and those obtained from a single-crystal $LaNiO_3$[53] are almost *one order of magnitude higher* than the other literature values. In general, the apparent electrical conductivity of a pressed/sintered material is heavily dependent on its relative density:[32,55] The apparent electrical conductivity varies from the inherent value of the material to almost an order of magnitude lower values as its relative density changes from 100% to 50%. The $LaNiO_3$ samples used in the cited studies in Fig. 3 except the single crystal were only pressed or sintered at around 1000 °C or lower[5,12,14,18,28,49,50,51,52,54] due to the poor thermal stability of $LaNiO_3$ under an ordinary partial pressure of oxygen (1 bar O_2 or less). Based on previous studies[12,49,51,56] and our recent study on the La–Ni–O system,[46] it is thought to be difficult to obtain fully dense samples (relative density over 95%) under such conditions. Therefore, the literature values of the electrical conductivity of $LaNiO_3$ are likely to be much underestimated due to the lower relative densities. It is worth mentioning that this large discrepancy cannot be attributed to the difference in the atmosphere where the electrical conductivity measurements were carried out, as the variation of the electrical conductivity of $LaNiO_3$ is less than 12% in the p_{O2} range of 10^{-3}–1 bar at 800 °C (see Fig. S1, ESI†).

The composition dependence of the electrical conductivity of $LaNi_{1-x}Fe_xO_3$ is proved to be monotonic. Fig. 4(a) and (b) shows the iron content dependence of the electrical conductivity of $LaNi_{1-x}Fe_xO_3$ at room temperature and 800 °C in 0.2 bar O_2. The electrical conductivity values at x = 0.4 obtained in this study agree reasonably with literature values. At $x < 0.4$, the electrical conductivity increases with decreasing x (increasing Ni content), reaching 1.0×10^4 S cm^{-1} and 2.5×10^3 S cm^{-1} at x = 0 at room temperature and 800 °C, respectively, while the literature data do not show a clear trend.¶,‖ This discrepancy

can be due to the underestimation of the conductivity of Ni-rich samples in the past studies due to the lower relative densities as discussed in the previous paragraph or the existence of secondary phases.[24,32] The increasing trend of the electrical conductivity with Ni content could be attributed to the previously proposed picture that the metal–insulator transition is driven by disorder effects arising from the substitution for Ni in metallic $LaNiO_3$ with Fe. However, further experimental and theoretical studies using appropriately synthesized samples are desirable to elucidate the nature of M–I transition in this system. Referring also to literature data on Ni-poor compositions, we can see that the electrical conductivity of $LaNi_{1-x}Fe_xO_3$ increases monotonically with decreasing x in the whole composition range.

In Fig. 5(a), the electrical conductivity of $LaNi_{1-x}Fe_xO_3$ is compared with those of simple perovskite or perovskite-related (layered-perovskite) oxides based on 3d transition metals Cr, Mn, Fe, Co, Ni, and/or Cu. These oxides are stable in air and at high temperatures ($\sim$500–800 °C), and have potential applications as the cathodes and interconnects of SOFCs. The electrical conductivity of $LaNiO_3$ ($LaNi_{1-x}Fe_xO_3$ with $x = 0$) is found to be the highest among the above oxides including popular cathode materials such as $La_{0.6}Sr_{0.4}Co_{0.2}Fe_{0.8}O_{3-\delta}$ (LSCF), $Ba_{0.5}Sr_{0.5}Co_{0.8}Fe_{0.2}O_{3-\delta}$ (BSCF), $La_{0.5}Sr_{0.5}MnO_{3-\delta}$ (LSM), and $La_{0.6}Sr_{0.4}CoO_{3-\delta}$ (LSC). More broadly, Fig. 5(b) compares the electrical conductivities of $LaNi_{1-x}Fe_xO_3$ and other representative electrically conducting oxides out of the above category, based on 3d, 4d, or 5d transition metals. ReO_3 exhibits 1–2 orders of magnitude higher conductivity than that of $LaNiO_3$. Also, RuO_2 with rutile structure, TiO_x ($x = \sim1$) with NaCl structure, Ti_2O_3 with corundum structure, and Na_xWO_3, $La_{1-x}Sr_xVO_3$, $SrMoO_3$, and $SrRuO_3$ with perovskite structure exhibit equal or higher conductivity than $LaNiO_3$. However, many of them (ReO_3,[60] NaCl-type TiO_x,[61] Ti_2O_3,[61] Na_xWO_3,[62,63] $La_{1-x}Sr_xVO_3$,[64,65] and $SrMoO_3$[66]) are unstable in high-temperature air and the rest of them ($SrRuO_3$ and RuO_2) are based on precious metal, both can be drawbacks for practical use. Therefore $LaNiO_3$ is now considered as the precious-metal-free oxide with the highest electrical conductivity in high-temperature air.

Conclusions

In conclusion, the electrical conductivity of Ni-rich $LaNi_{1-x}Fe_xO_3$ ($0 \le x \le 0.4$) is found to monotonically increase with decreasing x (increasing Ni content) at both room temperature and 800 °C by use of the fully dense single-phase polycrystalline samples prepared by the post-sintering oxidation process. The confirmed trend suggests that $LaNi_{1-x}Fe_xO_3$ with smaller x (higher Ni content) might be more suitable for the cathodes of SOFCs than the widely-studied composition $LaNi_{0.6}Fe_{0.4}O_3$ ($x = 0.4$). It should be noted, however, that a higher conductivity does not necessarily lead to a better electrode performance. Therefore, it is desirable to investigate the electrochemical properties of Ni-rich $LaNi_{1-x}Fe_xO_3$ ($0 \le x \le 0.4$). One concern with Ni-rich $LaNi_{1-x}Fe_xO_3$ is the thermal instability during operation at high temperatures,[35] but it may be less problematic for the applications in low-temperature SOFCs, which are under active development. In addition, Ni-rich $LaNi_{1-x}Fe_xO_3$ can be more readily applicable as oxygen electrodes in solid oxide electrolyzer cells (SOECs) because the electrodes are operated in highly oxidative conditions, where $LaNi_{1-x}Fe_xO_3$ is more stable.[38,46] (see Fig. S2, ESI†) Furthermore, in a broader context, $LaNiO_3$ is now considered as the precious-metal-free oxide with the highest electrical conductivity in high-temperature air (2.5×10^3 S cm^{-1} at 800 °C in 0.2 bar O_2) and can find other applications as an oxidation-resistant, high-temperature electrical conductor.

Conflicts of interest

There are no conflicts to declare.

Acknowledgements

This study was supported by Grant-in-Aid for JSPS Research Fellow Grant Number 16J09427. We are grateful to Shin-Etsu Chemical Co., Ltd for providing lanthanum oxide.

Notes and references

§ Fe may partially occupy the Ni-sites in $La_4Ni_3O_{10}$ and NiO.[44]

¶ Based on XRD patterns (Fig. 1), the amount of secondary phases (NiO and an unknown phase) is estimated to be $\sim$1 wt% or less. Therefore the secondary phases would not constitute a long-range conduction network and the high electrical conductivity observed in this study can be attributed to the main phase, $LaNi_{1-x}Fe_xO_3$. Also, the fact that the conductivity value of the $LaNiO_3$ polycrystal obtained in this study are almost identical to that of a single crystal at room temperature (Fig. 3(a)) suggests that the influence of secondary phases is not significant.

‖ In $LaNi_{1-x}Fe_xO_3$ ($0 \le x \le 0.4$) solid solutions, electronic conduction should dominate over ionic conduction. Although they contain oxygen vacancies[9,35,54] and can conduct oxide ions, the oxide ion conductivity at 800 °C is assumed to be less than 1 S cm^{-1} as in the case of other best oxide-ion-conducting perovskite oxides (LSC, LSGM, *etc.*).[90]

1 J. B. Goodenough, *Czech. J. Phys.*, 1967, **17**, 304–336.
2 C. N. R. Rao, O. Parkash and P. Ganguly, *J. Solid State Chem.*, 1975, **15**, 186–192.
3 O. Parkash, *Proc. Indian Natl. Sci. Acad., Part A*, 1978, **87**, 331–335.
4 K. Asai and H. Sekizawa, *J. Phys. Soc. Jpn.*, 1980, **49**, 90–98.
5 P. Ganguly, N. Y. Vasanthacharya and C. N. R. Rao, *J. Solid State Chem.*, 1984, **54**, 400–406.
6 J. B. Torrance, P. Lacorre, A. I. Nazzal, E. J. Ansaldo and C. Niedermayer, *Phys. Rev. B: Condens. Matter Mater. Phys.*, 1992, **45**, 8209–8212.
7 J. L. García-Muñoz, J. Rodríguez-Carvajal, P. Lacorre and J. B. Torrance, *Phys. Rev. B: Condens. Matter Mater. Phys.*, 1992, **46**, 4414–4425.
8 K. Sreedhar, J. M. Honig, M. Darwin, M. McElfresh, P. M. Shand and J. Xu, *et al.*, *Phys. Rev. B: Condens. Matter Mater. Phys.*, 1992, **46**, 6382–6386.

9 D. D. Sarma, O. Rader, T. Kachel, A. Chainani, M. Mathew and K. Holldack, *et al.*, *Phys. Rev. B: Condens. Matter Mater. Phys.*, 1994, **49**, 14238–14243.
10 T. Arima and Y. Tokura, *J. Phys. Soc. Jpn.*, 1995, **64**, 2488–2501.
11 G. Pari, S. Mathi Jaya, G. Subramoniam and R. Asokamani, *Phys. Rev. B: Condens. Matter Mater. Phys.*, 1995, **51**, 16575–16581.
12 A. Chainani, D. D. Sarma, I. Das and E. V. Sampathkumaran, *J. Phys.: Condens. Matter*, 1996, **8**, L631–L636.
13 W. H. Jung and E. Iguchi, *Philos. Mag. B*, 1996, **73**, 873–891.
14 N. E. Massa, H. Falcón, H. Salva and R. E. Carbonio, *Phys. Rev. B: Condens. Matter Mater. Phys.*, 1997, **56**, 10178–10191.
15 H. Falcón, A. E. Goeta, G. Punte and R. E. Carbonio, *J. Solid State Chem.*, 1997, **133**, 379–385.
16 D. D. Sarma, A. Chainani, S. R. Krishnakumar, E. Vescovo, C. Carbone and W. Eberhardt, *et al.*, *Phys. Rev. Lett.*, 1998, **80**, 4004–4007.
17 R. Kumar, R. J. Choudhary, M. Wasi Khan, J. P. Srivastava, C. W. Bao and H. M. Tsai, *et al.*, *J. Appl. Phys.*, 2005, **97**, 093526.
18 R. Funahashi, M. Mikami, S. Urata, M. Kitawaki, T. Kouuchi and K. Mizuno, *Meas. Sci. Technol.*, 2005, **16**, 70–80.
19 X.-D. Zhou, J. B. Yang, E.-C. Thomsen, Q. Cai, B. J. Scarfino and Z. Nie, *et al.*, *J. Electrochem. Soc.*, 2006, **153**, J133–J138.
20 K. Iwasaki, T. Ito, M. Yoshino, T. Matsui, T. Nagasaki and Y. Arita, *J. Alloys Compd.*, 2007, **430**, 297–301.
21 M. Wasi Khan, S. Husain, M. A. Majeed Khan, M. Gupta, R. Kumar and J. P. Srivastava, *Philos. Mag.*, 2010, **90**, 3069–3079.
22 E. Niwa, C. Uematsu, E. Miyashita, T. Ohzeki and T. Hashimoto, *Solid State Ionics*, 2011, **201**, 87–93.
23 E. Niwa, H. Maeda, C. Uematsu and T. Hashimoto, *Mater. Res. Bull.*, 2015, **70**, 241–247.
24 R. Chiba, F. Yoshimura and Y. Sakurai, *Proc. - Electrochem. Soc.*, 1999, **99-19**, 453–462.
25 V. V. Kharton, A. P. Viskup, E. N. Naumovich and V. N. Tikhonovich, *Mater. Res. Bull.*, 1999, **34**, 1311–1317.
26 R. N. Basu, F. Tietz, E. Wessel, H. P. Buchkremer and D. Stöver, *Mater. Res. Bull.*, 2004, **39**, 1335–1345.
27 H. Orui, K. Watanabe, R. Chiba and M. Arakawa, *J. Electrochem. Soc.*, 2004, **151**, A1412–A1417.
28 K. Świerczek, J. Marzec, D. Pałubiak, W. Zając and J. Molenda, *Solid State Ionics*, 2006, **177**, 1811–1817.
29 M. Bevilacqua, T. Montini, C. Tavagnacco, E. Fonda, P. Fornasiero and M. Graziani, *Chem. Mater.*, 2007, **19**, 5926–5936.
30 T. Komatsu, R. Chiba, H. Arai and K. Sato, *J. Power Sources*, 2008, **176**, 132–137.
31 T. Ohzeki, T. Hashimoto, K. Shozugawa and M. Matsuo, *Solid State Ionics*, 2010, **181**, 1771–1782.
32 R. Chiba, F. Yoshimura and Y. Sakurai, *Solid State Ionics*, 1999, **124**, 281–288.
33 N. Sukpirom, S. Iamsaard, S. Charojrochkul and J. Yeyongchaiwat, *J. Mater. Sci.*, 2011, **46**, 6500–6507.
34 J. Y. Chen, J. Rebello, V. Vashook, D. M. Trots, S. R. Wang and T. L. Wen, *et al.*, *Solid State Ionics*, 2011, **192**, 424–430.
35 R. A. Budiman, S. Hashimoto, T. Nakamura, K. Yashiro, K. Amezawa and T. Kawada, *ECS Trans.*, 2015, **66**, 177–183.
36 R. A. Budiman, T. Miyazaki, S. Hashimoto, T. Nakamura, K. Yashiro and K. Amezawa, *et al.*, *J. Electrochem. Soc.*, 2015, **162**, F1445–F1450.
37 V. V. Sereda, D. S. Tsvetkov, I. L. Ivanov and A. Y. Zuev, *J. Mater. Chem. A*, 2015, **3**, 6028–6037.
38 Y. Morishima, E. Niwa and T. Hashimoto, *J. Therm. Anal. Calorim.*, 2016, **123**, 1769–1775.
39 R. A. Budiman, H. J. Hong, S. Hashimoto, T. Nakamura, K. Yamaji and K. Yashiro, *et al.*, *Solid State Ionics*, 2017, **310**, 148–153.
40 K. Chen, H. Dai, S. He and L. Bi, *Fuel Cells*, 2018, **18**, 561–565.
41 N. Soltani, R. Martínez-Bautista, A. Bahrami, L. H. Arcos, M. Cassir and J. C. Carvayar, *Chem. Phys. Lett.*, 2018, **700**, 138–144.
42 Y. Chen, W. Zhou, D. Ding, M. Liu, F. Ciucci and M. Tade, *et al.*, *Adv. Energy Mater.*, 2015, **5**, 1500537.
43 E. A. Kiselev, N. V. Proskurnina, V. I. Voronin and V. A. Cherepanov, *Inorg. Mater.*, 2007, **43**, 167–175.
44 E. A. Kiselev and V. A. Cherepanov, *J. Solid State Chem.*, 2010, **183**, 1992–1997.
45 D. O. Bannikov and V. A. Cherepanov, *J. Solid State Chem.*, 2006, **179**, 2721–2727.
46 Y. Adachi, N. Hatada, K. Hirota, M. Kato and T. Uda, *J. Am. Ceram. Soc.*, 2019, **102**, 7077–7088.
47 Y. Adachi, N. Hatada, K. Hirota, M. Kato and T. Uda, *Abstracts of the 83rd Spring Meeting of the Electrochemical Society of Japan*, 2016, 1N20.
48 N. Hatada and T. Uda, *The 45th Symposium on Solid State Ionics of Japan Extended Abstracts*, 2019, 256–257.
49 I. F. Kononyuk, N. G. Surmach, S. P. Tolochko and T. V. Kugan, *Inorg. Mater.*, 1984, **20**, 1036–1039.
50 H. Nagamoto, I. Mochida, K. Kagotani, H. Inoue and A. Negishi, *J. Mater. Res.*, 1993, **8**, 3158–3162.
51 H. E. Höfer and R. Schmidberger, *J. Electrochem. Soc.*, 1994, **141**, 782–786.
52 R. D. Sánchez, M. T. Causa, J. Sereni, M. Vallet-Regí, M. J. Sayagués and J. M. González-Calbet, *J. Alloys Compd.*, 1993, **191**, 287–289.
53 J. Zhang, H. Zheng, Y. Ren and J. F. Mitchell, *Cryst. Growth Des.*, 2017, **17**, 2730–2735.
54 A. A. Yaremchenko, B. I. Arias-Serrano, K. Zakharchuk and J. R. Frade, *ECS Trans.*, 2019, **91**, 2399–2408.
55 J. Mizusaki, S. Tsuchiya, K. Waragai, H. Tagawa, Y. Arai and Y. Kuwayama, *J. Am. Ceram. Soc.*, 1996, **79**, 109–113.
56 H. Obayashi and T. Kudo, *Jpn. J. Appl. Phys.*, 1975, **14**, 330–335.
57 I. Wærnhus, T. Grande and K. Wiik, *Solid State Ionics*, 2005, **176**, 2609–2616.
58 A. Berenov, E. Angeles, J. Rossiny, E. Raj, J. Kilner and A. Atkinson, *Solid State Ionics*, 2008, **179**, 1090–1093.
59 E. A. Kiselev and V. A. Cherepanov, *Solid State Ionics*, 2011, **191**, 32–39.
60 H. Oppermann, *Z. Anorg. Allg. Chem.*, 1985, **523**, 135–144.

61 M. Cancarevic, M. Zinkevich and F. Aldinger, *CALPHAD: Comput. Coupling Phase Diagrams Thermochem.*, 2007, **31**, 330–342.
62 M. E. Straumanis, *J. Am. Chem. Soc.*, 1949, **71**, 679–683.
63 F. H. Potter and R. G. Egdell, *J. Mater. Chem.*, 1994, **4**, 1647–1651.
64 T. Nakamura, G. Petzow and L. J. Gauckler, *Mater. Res. Bull.*, 1979, **143**, 649–659.
65 R. Pankajavalli and O. M. Sreedharan, *Mater. Lett.*, 1995, **24**, 247–251.
66 T. Maekawa, K. Kurosaki, H. Muta, M. Uno and S. Yamanaka, *J. Alloys Compd.*, 2005, **390**, 314–317.
67 I. Yasuda and T. Hikita, *J. Electrochem. Soc.*, 1993, **140**, 1699–1704.
68 J. Mizusaki, Y. Yonemura, H. Kamata, K. Ohyama, N. Mori and H. Takai, *et al.*, *Solid State Ionics*, 2000, **132**, 167–180.
69 P. Ried, P. Holtappels, A. Wichser, A. Ulrich and T. Graule, *J. Electrochem. Soc.*, 2008, **155**, B1029–B1035.
70 Y. Adachi, N. Hatada and T. Uda, *J. Electrochem. Soc.*, 2016, **163**, F1084–F1090.
71 H.-C. Yu and K.-Z. Fung, *Mater. Res. Bull.*, 2003, **38**, 231–239.
72 S. Yoo, S. Choi, J. Kim, J. Shin and G. Kim, *Electrochim. Acta*, 2013, **100**, 44–50.
73 M. Al Daroukh, V. V. Vashook, H. Ullmann, F. Tietz and I. Arual Raj, *Solid State Ionics*, 2003, **158**, 141–150.
74 S. Takahashi, S. Nishimoto, M. Matsuda and M. Miyake, *J. Am. Ceram. Soc.*, 2010, **93**, 2329–2333.
75 Q. Li, H. Zhao, L. Huo, L. Sun, X. Cheng and J.-C. Grenier, *Electrochem. Commun.*, 2007, **9**, 1508–1512.
76 H.-I. Yoo, *J. Mater. Res.*, 1989, **4**, 23–27.
77 S. P. Denker, *J. Appl. Phys.*, 1966, **37**, 142–149.
78 J. M. Honig and T. B. Reed, *Phys. Rev.*, 1968, **174**, 1020–1026.
79 H. Kuwamoto, J. M. Honig and J. Appel, *Phys. Rev. B: Condens. Matter Mater. Phys.*, 1980, **22**, 2626–2636.
80 P. B. Allen, R. M. Wentzcovitch, W. W. Schulz and P. C. Canfield, *Phys. Rev. B: Condens. Matter Mater. Phys.*, 1993, **48**, 4359–4363.
81 W. D. Ryden, A. W. Lawson and C. C. Sartain, *Phys. Lett. A*, 1968, **26**, 209–210.
82 P. A. Miles, W. B. Westphal and A. von Hippel, *Rev. Mod. Phys.*, 1957, **29**, 279–307.
83 O. A. Marina, N. L. Canfield and J. W. Stevenson, *Solid State Ionics*, 2002, **149**, 21–28.
84 A. A. Yaremchenko, B. Brinkmann, R. Janssen and J. R. Frade, *Solid State Ionics*, 2013, **247–248**, 86–93.
85 J. B. Webb and M. Sayer, *J. Phys. C: Solid State Phys.*, 1976, **9**, 4151–4164.
86 L. H. Brixner, *J. Inorg. Nucl. Chem.*, 1960, **14**, 225–230.
87 P. B. Allen, H. Berger, O. Chauvet, L. Forro, T. Jarlborg and A. Junod, *et al.*, *Phys. Rev. B: Condens. Matter Mater. Phys.*, 1996, **53**, 4393–4398.
88 L. D. Ellerbeck, H. R. Shanks, P. H. Sidles and G. C. Danielson, *J. Chem. Phys.*, 1961, **35**, 298–302.
89 T. P. Pearsall and C. A. Lee, *Phys. Rev. B: Condens. Matter Mater. Phys.*, 1974, **10**, 2190–2194.
90 V. V. Kharton, F. M. B. Marques, J. A. Kilner and A. Atkinson, in *Solid State Electrochemistry I*, ed. V. V. Kharton, Wiley-VCH Verlag GmbH & Co. KGaA, Weinheim, Germany, 2009, ch. 9, pp. 301–334.